CHEMISTRY
A EUROPEAN JOURNAL

DOI: 10.1002/chem.201000866

Contributions of Electron Microscopy to Understanding CO Adsorption on Powder Au/Ceria–Zirconia Catalysts

José María Cíes,[a] Juan José Delgado,[a] Miguel López-Haro,[a] Ratchaneekorn Pilasombat,[b, c] José Antonio Pérez-Omil,[a] Susana Trasobares,[a] Serafin Bernal,[a] and José Juan Calvino*[a]

Dedicated to Professor Serafin Bernal on the occasion of his retirement

Abstract: The influence of the highly dispersed gold phase on the CO–support interaction occurring in two 2.5 wt% $Au/Ce_{0.62}Zr_{0.38}O_2$ catalysts with medium (Au/CZ-MD) and high (Au/CZ-HD) metal dispersion is quantitatively assessed. For this purpose, we have followed an approach in which high-angle annular dark-field scanning transmission electron microscopy (HAADF-STEM), computer modelling, volumetric adsorption and FTIR spectroscopy studies are combined. This approach has already been fruitfully applied to the investigation of the specific CO–metal adsorption in Au/ceria–zirconia catalysts. As deduced from the experimental studies reported herein, the presence of gold dramatically increases the amount of CO strongly chemisorbed on the support. Moreover, this amount is sensitive to the metal dispersion, thus suggesting the occurrence of a mechanism in which the CO molecules that are initially adsorbed on the gold nanoparticles are further transferred to the support by means of a spillover process. An annular model is proposed for the growth of the CO phase adsorbed on the ceria–zirconia mixed oxide in the presence of Au. By assuming this model, we have estimated the width of the annulus, Δr, of the adsorbed CO grown around the Au nanoparticles in Au/CZ-MD and Au/CZ-HD catalysts. This value is found to be very close to $\Delta r \approx 2$ nm in both cases, the coincidence lending some additional support to the model. To further confirm this proposal, we have investigated the influence of CO pre-adsorption on the D_2–Au/CZ-MD interaction, at 298 K. As revealed by FTIR spectroscopy, the kinetics of the deuterium spillover is significantly disturbed by the pre-adsorbed CO, which is fully consistent with an annular model for the CO adsorption. We conclude from the global analysis of the results reported here and those already available on CO–Au adsorption that the appropriate combination of nanostructural, computer modelling and chemical techniques is a powerful tool allowing us to gain a comprehensive picture of the complex series of processes involved in the CO adsorption on this relevant family of gold catalysts.

Keywords: adsorption · carbon monoxide · electron microscopy · gold · supported catalysts

[a] J. M. Cíes, Dr. J. J. Delgado, M. López-Haro, Dr. J. A. Pérez-Omil, Dr. S. Trasobares, Dr. S. Bernal, Dr. J. J. Calvino
Departamento de Ciencia de los Materiales e Ingeniería Metalúrgica y Química Inorgánica
Facultad de Ciencias, Universidad de Cádiz,
11510 Puerto Real, Cadiz (Spain)
Fax: (+34) 956-016288
E-mail: jose.calvino@uca.es

[b] Dr. R. Pilasombat
Center for Theory and Application of Catalysis (CenTaCat)
School of Chemistry and Chemical Engineering
Queen's University Belfast, Belfast, BT9 5AG (UK)

[c] Dr. R. Pilasombat
Current address: Department of Chemistry
Mahasarakham University, Kantharawichai District
Mahasarakham 44150 (Thailand)

Introduction

Catalysts consisting of gold nanoparticles supported on ceria and ceria-containing mixed oxides are known to be highly active materials for a number of reactions involving CO, such as CO oxidation[1–10] and low-temperature water gas-shift reactions.[11–21] Despite their high activity, under reaction conditions, these materials may often undergo significant deactivation problems[5,8,9,12,15,17–19,21]. This is a major, very challenging, issue, which is actually limiting their practical applications.[13,15] Though far from being well understood, a number of factors have been suggested to cause these deactivation effects[5,8,9,12,13,15,17–19]. Among them, several authors have agreed on the relevant role played by the

support carbonation.[12,17,21,22] To clarify this point, an in-depth understanding of the CO adsorption processes occurring on both the gold nanoparticles and the ceria-based supports, and the eventual relationship existing between them, should therefore be considered as an important research target.

Our laboratory[23] has recently developed an approach that has proved to be very powerful for investigating the CO adsorption specifically taking place on gold nanoparticles supported on powdered ceria–zirconia mixed oxides. By combining in an appropriate manner high-resolution transmission electron microscopy (HRTEM), high-angle annular dark-field scanning transmission electron microscopy (HAADF-STEM), computer modelling, FTIR spectroscopy and volumetric CO adsorption studies, we have been able to show in ref. [23] that the chemical principles governing the CO–Au interaction, at 308 K, under adsorbate partial pressures ranging from 0 to 300 torr, are similar to those proposed earlier for model gold single-crystal systems on the basis of experimental studies carried out at far lower temperature and CO partial pressures.[24] In effect, as discussed in ref. [23] on conventional powdered Au/ceria–zirconia catalysts, under the above-mentioned experimental conditions, the CO adsorption sites consist of surface Au atoms showing coordination number ≤ 7.

To further investigate the chemistry of the CO–(Au/ceria–zirconia) systems, in this work, the approach described in ref. [23] is applied to the investigation of the CO adsorption specifically occurring on the support. Our experimental studies have been performed on both the bare support and two Au(2.5 wt %)/$Ce_{0.62}Zr_{0.38}O_2$ catalysts showing significantly different metal-nanoparticle size distributions. As deduced from the results presented and discussed below, the kinetics of the CO adsorption of the ceria–zirconia mixed oxide is dramatically modified by the presence of highly dispersed gold. Consequently to this, on our Au/ceria–zirconia samples, the amount of CO specifically chemisorbed on the support strongly increases with reference to that determined for the pure mixed oxide. Moreover, our results indicate that this amount is sensitive to the metal dispersion, so that the higher the gold dispersion the larger the amount of CO adsorbed on the support.

To interpret all the observations given above, an annular model for the growth of the adsorbed CO phase on the ceria–zirconia mixed oxide in our gold catalysts is proposed. In accordance with this, the CO adsorption would take place first on the metal nanoparticles, the resulting CO species being further transferred to the support through a spill-over-like process. In our model, the total amount of CO finally adsorbed on the support would be determined by the surface diffusion of the spilled-over species. This model is further confirmed by a FTIR study of deuterium spillover carried out on catalysts either pretreated or un-pretreated with CO. As deduced from this study, the CO pre-adsorption disturbs very significantly the deuterium spillover process.

Results and Discussion

HAADF-STEM study of the gold dispersion: Two gold catalysts supported on a $Ce_{0.62}Zr_{0.38}O_2$ mixed oxide with 2.5 wt % metal loading have been studied. To establish the particle size distribution in these catalysts, high-angle annular dark-field images recorded in scanning transmission electron microscopy mode (HAADF-STEM) were obtained (Figure 1).

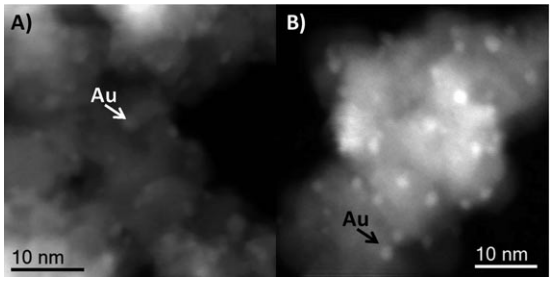

Figure 1. HAADF-STEM images of A) Au/CZ-MD and B) Au/CZ-HD catalysts.

In this imaging mode, which has been fruitfully applied to investigate in detail the structure of a variety of gold catalysts,[23,25–27] an annular detector is used to collect those electrons that have been scattered at high angles at each point of the scanned area of the sample. The quite interesting feature of this process is that the number of electrons scattered at high angle shows a direct correlation with the squared value of the average atomic number (Z) of the region crossed by the electron beam.[28] Therefore, regions of the material in which the average atomic number of the elements is high will appear in the image as very bright points, whereas those in which the average Z is small are imaged as lower intensity areas. Thus, contrasts in STEM-HAADF images provide information about the spatial distribution of elements in the imaged areas.

By considering the atomic number of the elements involved in the catalysts we have investigated ($Z_{Au}=79$, $Z_{Ce}=58$, $Z_{Zr}=40$ and $Z_O=8$) it becomes clear that the brighter areas in the images presented in Figure 1 are those corresponding to Au. Note how gold is present in the form of nanoparticles, some marked with arrows, the diameters of which can be directly estimated from the contrasts in these images.

By measuring a sufficiently high number of particles (above 250) on different STEM-HAADF images, reliable particle size distributions could be obtained for the two catalysts (Figure 2). These distributions can be processed to estimate the total dispersion of gold, D ($D=100\times(Au_S/Au_T)$, in which Au_T = total number of gold atoms and Au_S = total number of gold atoms at the surface of the nanoparticles) in both catalysts. Table 1 (column 2) includes these estimations assuming a truncated-cuboctahedral shape for the metal nanoparticles, which is the morphology better fitting the ex-

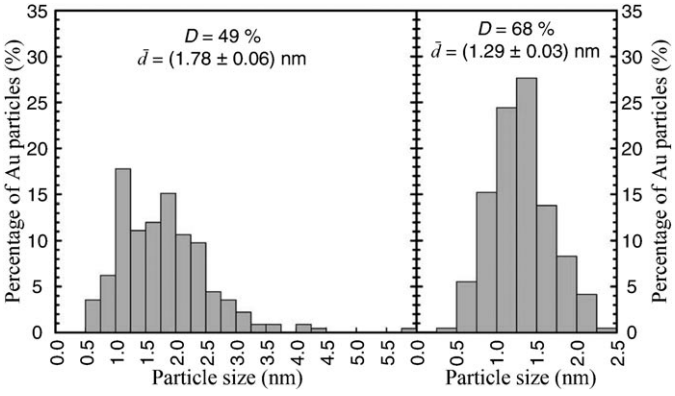

Figure 2. Particle size distributions of Au/CZ-MD (left) and Au/CZ-HD (right) catalysts.

Table 1. Dispersion and quantitative CO chemisorption data.

Sample	D [%]	CO-CZ [μmol g^{-1}]	θ_{111} [%]	r_i [nm]
CZ	–	6	1.4	–
Au/CZ-MD	49	100	23.0	1.9
Au/CZ-HD	68	220	50.7	1.7

perimental high-resolution electron microscopy (HREM) images recorded for them.[23]

Note that the two catalysts display significant differences in their Au nanoparticle size distributions. One of them is characterised by an average gold particle diameter of (1.79 ± 0.06) nm and a total dispersion value of $D = 49\,\%$, whereas the second, with a narrower distribution, presents a smaller average particle diameter, (1.30 ± 0.03) nm, and a much higher total dispersion, $D = 68\,\%$. In the following we will refer to these samples as Au/CZ-MD (medium-dispersion catalyst) and Au/CZ-HD (high-dispersion catalyst), respectively.

Volumetric study of CO adsorption on Au/CZ and CZ samples: Volumetric CO chemisorption on the two Au/CZ catalysts and the ceria–zirconia mixed oxide sample used as support were performed at 308 K. The experimental routine was the same as that already applied in refs. [23] and [29]. Two consecutive isotherms separated by 30 min evacuation (residual pressure better than 1×10^{-6} torr) at 308 K were recorded for the three investigated samples. As shown in ref. [29] on the basis of FTIR studies, the first isotherm accounts for the total amount of CO adsorbed on both the gold nanoparticles and the support. Adsorption on the support takes place in the form of weakly bonded species on top of the metal cations and also through the formation of strongly bonded species.[29] The 30 min evacuation treatment at 308 K removes CO adsorbed on gold and also the weakly bonded CO on the support; the only species remaining chemisorbed after this evacuation treatment are those strongly bonded to the ceria–zirconia support. As shown in ref. [29] these latter forms mainly consist of carbonate species.

Thus, the amount of CO adsorbed in a second isotherm onto the metal/support system would account specifically for CO adsorbed on the metal nanoparticles and the weakly bonded CO on support cations.

The latter contribution of weak adsorption can be estimated from isotherms of the bare support. As it is the case in the metal/support system, a first isotherm also contributes to both weakly and strongly CO adsorbed species. Since the first adsorption type is evacuated at 308 K, a second isotherm after this treatment provides the amount of CO adsorbed onto the bare support cations.

Therefore, from appropriate differences between these isotherms, the total amount of adsorbed CO can be split into the specific contribution of CO adsorbed onto the metal nanoparticles and onto the support.

Figure 3, which shows plots of the results of a volumetric CO chemisorption study on the Au/CZ-MD system, illustrates the procedure mentioned above. The lines of solid circles and solid triangles in Figure 3A correspond to the first and second isotherms recorded on the Au/CZ-MD catalyst. The line at the bottom (solid squares) corresponds to the second isotherm on the CZ support, as mentioned before,

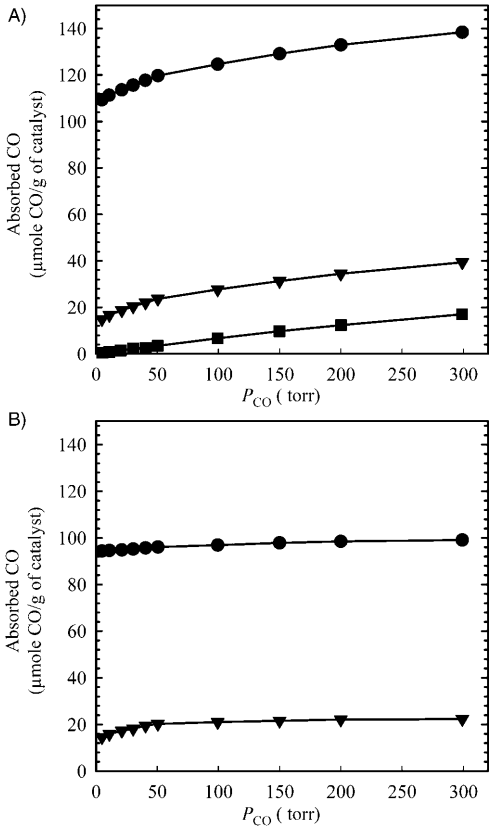

Figure 3. A) Volumetric CO adsorption isotherms: (●) first isotherm on the Au/CZ-MD catalyst; (▼) second isotherm on Au/CZ-MD; (■) second isotherm on the bare CZ support. B) Specific CO adsorption on the metal (▼) and on the support (●) obtained by using differences between isotherms plotted in Figure 3A.

which is that depicting specifically the evolution with CO pressure of species weakly bonded to the support. From these three isotherms two differences can be calculated (Figure 3B): 1) by taking the difference between the first and second isotherm on Au/CZ-MD, we get the isolated contribution of strongly adsorbed CO species onto the support (plotted in the form of solid dots); 2) the component corresponding to CO specifically attached to the gold particles (solid triangles), by the difference between the second isotherms of Au/CZ-MD and CZ.

Note how the isotherm corresponding to adsorption on gold becomes flat at CO pressures around 100 torr, conditions at which saturation of the metal-particle adsorbing sites seems to have occurred. From these saturation values, CO/Au ratios can be estimated. For the Au/CZ-MD catalyst the CO/Au ratio at saturation is 0.19, whereas it increases up to 0.47 for the Au/CZ-HD one. Changes in the particle size distributions between these two catalysts, commented on above, can precisely account for this difference. Moreover, the application of the methodology developed in ref. [23] has allowed us to confirm that the CO/Au values reported for the HD and MD catalysts are fairly consistent with the proposal that CO adsorption on the metal takes place on gold surface atoms showing a coordination number ≤ 7.

This is very relevant information that can be extracted from the analysis of these isotherms, but a more thorough consideration can also provide quite interesting features related to the CO adsorption onto the support. As clearly deduced from the inspection of Figure 3B, the largest contribution to the total amount of CO adsorbed on the Au/CZ-MD catalyst is that associated with the forms strongly chemisorbed on the support. Its evaluation is therefore critically important to fully understand the CO–catalyst interaction.

Figure 4 shows the evolution with pressure of the CO adsorbed onto the support for the two gold catalysts and on the bare ceria–zirconia support used to prepare these catalysts. A number of aspects are worth being commented on. Note first that in the catalyst samples, a steady amount of adsorbed CO is reached at very low pressures, below 50 torr. In the case of the bare support only a very slight increase in the amount of adsorbed CO is observed with increasing pressure, but in any case the difference between the values recorded at the lowest and highest pressures does not exceed 4 μmol.

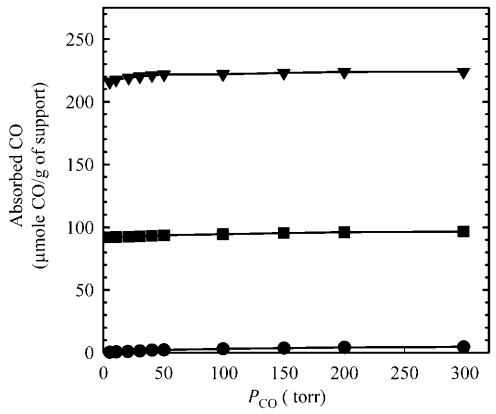

Figure 4. CO adsorption on the support observed for Au/CZ-MD (■), Au/CZ-HD (▼) and the bare CZ support (●).

More important, note how the amount of CO adsorbed per gram of oxide observed on the two catalysts is much higher than that corresponding to the bare support, even at the highest CO pressures. This result indicates that the presence of the metal nanoparticles very much enhances the CO adsorption on the support . To our knowledge, no quantitative data are presently available on this remarkable effect.

Finally, it is worth highlighting that the amount, per gram of support, of spilt-over CO is very different in the two catalysts, about 100 μmol in AuCZ-MD and 220 μmol in AuCZ-HD (Table 1, third column). These data prove, therefore, a direct relationship between the metal-particle size distribution and the total amount of CO adsorbed on the support.

Nanostructural model for CO adsorption onto the support: We have investigated in more detail the correlation between these two parameters: the amount of CO strongly chemisorbed on the support and metal-particle size distribution. In particular, our goal has been to devise a structural model that would allow us to explain in quantitative terms, as already done with the adsorption on the metal particles, the CO chemisorption on the ceria–zirconia support.

A structural parameter that follows a direct correlation with dispersion is the value of the total perimeter of the metal-nanoparticle–support interface. Starting from this idea, we could guess that CO spills over to the support, through the metal atoms at the nanoparticle perimeter, and then diffuses away on the surface until it reaches a certain maximum distance. A process like this would finally give rise to a situation in which each metal nanoparticle would be surrounded by an annulus of adsorbed CO species, as sketched in Figure 5.

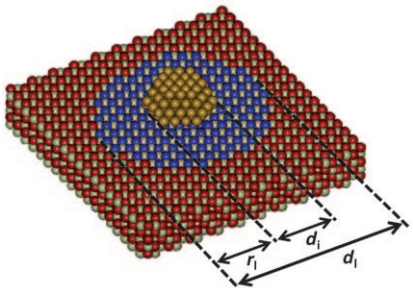

Figure 5. Nanostructural model proposed for the CO spillover onto the CZ support. The blue spheres depict the location of the surface oxygen atoms involved in the formation of carbonates.

If the diffusion ability of the CO molecules on the surface of the support is assumed to be constant, independent of the diameter of the gold metal particle from which they spilt

over, that is, we can assume a constant diffusion limit radius (r_l), the support surface area within the annular region of one particle would depend on its two characteristic diameters: the inner diameter, which would be just that of the metal particle (d_i) and its outer diameter, which would be given by Equation (1):

$$d_l = d_i + 2r_l \quad (1)$$

The area covered by spilt-over CO around each particle (A_i) would then be given by Equation (2):

$$A_i = \frac{\pi}{4}(d_l^2 - d_i^2) \quad (2)$$

The total area of the support covered by CO around all the particles included in one particle size distribution (A_D) could be then obtained by adding the contribution of each particle diameter, as follows [Eq. (3)]:

$$A_D = \sum_i P_i \cdot A_i \quad (3)$$

in which P_i stands for the percentage of particles in class i of the particle size distribution.

Finally, to obtain the total area covered in the catalyst by CO, per gram of support, A, we would have to estimate the number of times, F, we need to reproduce the particle size distribution to account for the total metal loading. This can be done by calculating the total number of atoms included in the particle size distribution. This last number can be calculated from the metal particle model and the diameters of each particle included in the particle size distribution. Once F has been estimated, we could then write [Eq. (4)]:

$$A = A_D \cdot F \quad (4)$$

Note that the result of all these calculations will finally depend on the exact value at which we set r_l. Therefore, to determine experimentally the value of this parameter for a particular catalyst we only have to choose the value that fits with the observed total CO coverage data. To do so, we have to calculate first the amount of support surface area covered by CO in that catalyst, A_{CO}.

Given that FTIR data of adsorbed CO indicates that the irreversible forms of adsorbed CO correspond to carbonate-like species, the adsorption on the support of one CO molecule must involve the interaction with two surface oxygen atoms. Therefore, the total support area involved in the interaction with CO will depend on the number of oxygen atoms per unit surface area. This value can be estimated from the crystallographic parameters of the support oxide and by assuming a particular crystallography for the exposed support surfaces.

Given that the {111} facets are, thermodynamically, the most stable in these oxides,[30] we will assume, for the sake of simplicity, that this represents the only contribution in our case. For a ceria–zirconia oxide like the one used in our experiments, the number of oxygen atoms per square nanometer in {111} facets is given by $\sigma_{111} = 8.3$.

Although changing the surface composition to a more complex mixture of {*hkl*} facets will slightly affect the result of our calculations, the most general conclusions to be shown later will not be affected at all, because we are comparing the results obtained on two different catalysts prepared on the same oxide support. Moreover, quite recent STEM-HAADF electron tomography experiments[27] have proved that a significant number of metal nanoparticles in gold catalysts prepared by the same procedure used here, precipitation–deposition, locate preferentially on sites that allow a large contact with {111} facets, these being therefore preferred anchoring sites for the metal particles.

Using the oxygen surface-density value for {111} facets mentioned above (σ_{111}), we can translate the total amount of CO adsorbed onto the support (m_{CO}), in micromoles, into a total covered surface, A_{CO}, as follows [Eq. (5)]:

$$A_{CO} = \frac{2N_A \times 10^{-6} m_{CO}}{\sigma_{111}} \quad (5)$$

To fix the limit of the diffusion distance, we only have to increase in small steps the value of r_l and calculate the corresponding value of A, until this parameter becomes equal to A_{CO}. By using this approach, the values of r_l estimated for Au/CZ-MD and Au/CZ-HD catalysts studied here were 1.9 and 1.7 nm, respectively (Table 1, last column).

Note that these values are very close to each other, as expected for measurements performed on catalysts based on the same support and at the same adsorption temperature. The good agreement between these two values provides in fact an indication of the adequacy of the structural model we are proposing. A significant deviation would have meant that the ability of CO to migrate onto the surface of both catalysts should have been different, which in this case does not seem reasonable.

Once these r_l values are determined we can also estimate the fraction of the total surface area of the support that becomes covered with the spilt-over CO, θ_{111}. As shown in Table 1, for AuCZ-MD and AuCZ-HD this parameter takes the following values, respectively: 23.0 and 50.7%. As we noted previously, the total amount of CO adsorbed onto the support in the catalyst with a high metal dispersion was roughly 2.2 times higher than that observed in the catalyst with the lower dispersion, and this is correspondingly reflected in the support coverage values. Note, however, that in both catalysts most of the surface is not affected by coverage with carbonates. This behaviour of CO adsorption contrasts clearly with that observed for hydrogen adsorption.[29] In the latter, quantitative estimations of the extension of spillover indicate that a full coverage of the ceria–zirconia surface is reached when hydrogen is adsorbed onto these catalysts at the same temperature and within the same total pressure range. This is quite an interesting difference to note, as it can be used, as we will show later, to further prove the validity of the CO adsorption model proposed here.

Figure 6 shows plots of the evolution of total coverage of the CZ support by spillover CO as a function of particle size (bottom axis). Note that although there is a large difference between the total CO adsorbed by the two catalysts, the total coverage in both cases is, as mentioned before, far below 100%. Moreover, note how the smaller particles, mostly below 3 nm, represent the major sources of spillover CO. In the high-dispersion catalysts, Au/CZ-HD, such particles correspond to the total amount of gold in the catalyst (upward lines, top axis) but they are only less than 75% of the total gold atoms in the catalyst with medium dispersion, Au/CZ-MD (downward lines, top axis). Therefore, though larger particles may comprise a significant fraction of the total number of metal atoms, they do not largely contribute to the total CO adsorbed onto the support.

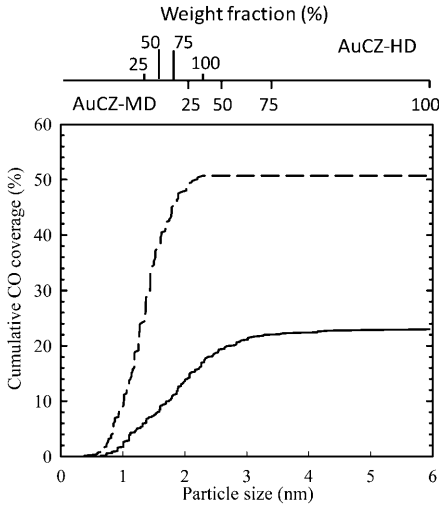

Figure 6. Cumulative CO coverage, as a function of gold particle size, for AuCZ-MD (solid line) and AuCZ-HD (dashed line) catalysts. The lines on the top axis show the evolution of the weight fraction of gold atoms in the two catalysts as a function of particle size.

FTIR study of deuterium spillover: To give some further support to the annular model developed herein for the strong CO adsorption on the ceria–zirconia mixed oxide in the presence of the supported gold phase, we have run an additional experiment aimed at investigating the influence of CO preadsorption on the Au/CZ-MD catalysts on the kinetics of the deuterium spillover.

As shown in ref. [29], hydrogen spillover on Au/CZ, even at 298 K, is rather fast. The question is whether the CO preadsorption, with inherent formation of a carbonated ring surrounding the gold nanoparticles, could affect the kinetics of this process. To evaluate this effect, two D_2 chemisorption experiments were performed on the Au/CZ-MD catalyst. In the first experiment, this catalyst was submitted to the standard oxidising pretreatment at 523 K that we have routinely applied as a cleaning procedure throughout all of this work. The second one was run after treating the pre-cleaned catalyst with CO (40 torr), at 298 K for 1 h, and further evacuation for 30 min at 298 K. The latter step was aimed at ensuring that gold nanoparticles were free from chemisorbed CO which, as deduced from the CO and H_2 co-adsorption experiments reported in ref. [29], could disturb the activation of the H_2 (D_2) molecule by the metal, which is the first step of the spillover process. After completing the above-mentioned pretreatments, the samples were contacted in both cases with D_2 (40 torr), at 298 K, and a time-resolved series of FTIR spectra were recorded for them.

Figure 7 shows a summary of the spectra recorded in the two regions that are relevant in this study, those corresponding respectively to the stretching modes of O–D (2800–2200 cm^{-1}) and to the carbonate–carboxylate range (1750–1100 cm^{-1}). The upper part of Figure 7 accounts for the spectra recorded on the sample just submitted to the cleaning pretreatment, whereas the bottom part deals with the study carried out on the sample further treated with CO. In both cases, spectra at $t=0$ min correspond to the samples before any contact with D_2.

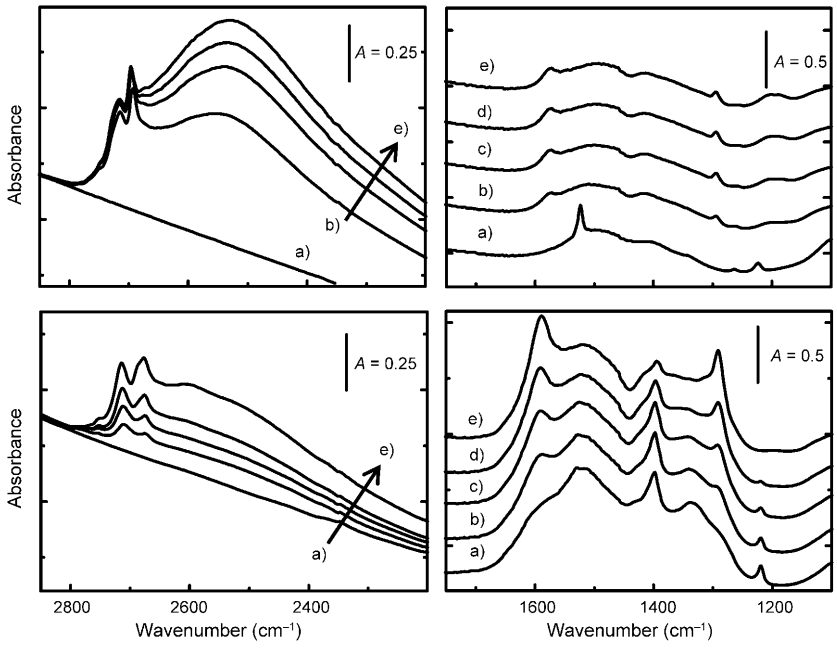

Figure 7. FTIR study of the D_2 interaction with the pre-cleaned Au/CZ-MD sample (top) and after exposure to a CO atmosphere (bottom). The spectra of a) the initial sample and samples after b) 5, c) 15, d) 30 and e) 60 min under D_2 are included.

Regarding the ν(OD) region, the spectra recorded for both samples mainly consist of two well-resolved bands occurring on the high-frequency side, which may be assigned to free O–D groups in different surface environments, and a very broad feature centred at approximately 2600 cm^{-1} typically interpreted to be due to bridged O–D forms. There are, however, some significant differences between the spectra shown in the upper and bottom parts of Figure 7, respectively. In the case of the pre-cleaned catalyst (upper part), the intensity of the bands grows up very rapidly, an apparent saturation of the spectrum being reached after 30 min of exposure to D_2. By contrast, on the sample additionally treated with CO (bottom part), the evolution with time of the spectra is much slower, and the intensity of the spectrum recorded after 30 min of contact with deuterium is much lower. This idea is quantitatively assessed in Figure 8, in

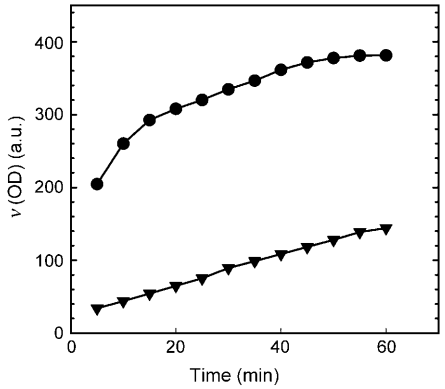

Figure 8. Evolution with time of the O–D integrated absorbance data (2800–2200 cm^{-1}) observed during the exposure to D_2 (40 torr): (●) on the pre-cleaned AuCZ-MD catalyst and (▼) on the same catalysts pretreated with CO before exposure to deuterium.

which the evolution with time of the integrated absorption data for the ν(OD) bands reported in Figure 7 is plotted. Though the deuterium spillover is not completely inhibited on the catalyst pretreated with CO, Figure 8clearly shows that its rate is much lower than that observed on the clean sample, un-pretreated with CO.

Regarding the observation commented on above, it is worth recalling that, in accordance with the volumetric data, the support fraction free from carbonate species in the Au/CZ-MD sample represents as much as 78% of its overall surface area. Therefore, the different intensity of the ν(OD) spectra recorded for catalysts pretreated and un-pretreated with CO cannot be interpreted in terms of unavailability of the support surface, but it rather suggests a very significant perturbation of the kinetics of the spillover process. This perturbation seems to be due to an efficient barrier effect played by the carbonate species localised within the annulus surrounding the metal nanoparticles.

The growth with time of the bands at 1589 and 1290 cm^{-1} in Figure 7 (bottom), which can be attributed to the formation of formate species,[31] suggests the interaction of the spilt-over deuterium with the carbonates around the metal particles, during its necessary transfer through the carbonate annulus, before reaching the free areas of the support. Such a modification of the mechanism could explain the observed perturbation of the kinetics of the deuterium spillover process, thus giving further support to the annular model proposed in this work.

Conclusion

With the appropriate combination of electron microscopy, computer modelling and chemical techniques, we have developed a methodology that has proved to be a very powerful tool for gaining a rather detailed picture of the complex interactions occurring between CO and both the dispersed gold phase and the ceria–zirconia mixed oxide support, under temperature and CO partial pressure conditions close to those at which the catalytic processes are run.

Our approach has allowed us to determine, on a quantitative basis, the specific contributions of both the metal and support to the overall CO adsorption process. Moreover, the results reported here, like those already shown in ref. [23] suggest that the chemical properties of the supported gold nanoparticles may be interpreted in similar terms to those earlier proposed for model single-crystal systems.[24] Regarding the CO adsorption on the ceria–zirconia support, the results discussed in this work clearly show that the supported gold phase plays a key role in the process, the amount of adsorbed CO being much larger in the presence of the metal. Likewise, it has been unequivocally shown that, on Au/CZ catalysts, this amount is strongly dependent on the metal dispersion, thus indicating that, in the presence of a supported gold phase, the very first step of the process consists of the adsorption of the CO molecules on the metal that are further transferred to the support. This leads to an annular model for the adsorption. From our study, an average width of about 2.0 nm could be estimated for the ring of carbonate species formed around the metal nanoparticles. The proposed model is also consistent with results of a FTIR study on the deuterium spillover process on surfaces of Au/CZ samples that are either clean or carbonated by CO pre-adsorption.

Let us finally recall that the use of STEM-HAADF images have been crucial to establish reliable metal-particle size distributions, which provide the basic support to the CO adsorption models proposed for both the gold nanoparticles and the ceria–zirconia mixed oxide. As shown here, this electron microscopy technique becomes of major importance in the nanostructural characterisation of metal catalysts, like those studied here, dispersed over the surface of supports involving elements with high atomic number, as it is the case of ceria–zirconia oxides.

Experimental Section

A $Ce_{0.62}Zr_{0.38}O_2$ mixed oxide, kindly donated by Grace Davison, with a BET surface area of 63 $m^2 g^{-1}$ was used as the support in the present study. No big changes were observed in the textural properties after gold deposition. A high-dispersion gold catalyst (Au-CZ-HD) was obtained by using a deposition–precipitation method using sodium carbonate as the precipitating agent and the preparation procedure described in ref. [29]. A medium gold dispersion was obtained by using urea as the precipitating agent and the synthesis method reported in ref. [32]. In both cases, the gold precursor was 99.99% $H[AuCl_4]$, from Alfa Aesar, and they were calcined at 250 °C in a 5% O_2/He flow. The final metal loading, confirmed by ICP analysis, was 2.5% for both catalysts.

HAADF-STEM images were recorded on a JEOL2010F instrument by using an electron probe (0.5 nm diameter) at a diffraction camera length of 10 cm. HREM images were recorded on the same microscope with 0.19 nm spatial resolution.

Volumetric adsorption experiments, N_2 physisorption at 77 K, and CO chemisorption at 308 K, were performed on a Micromeritics ASAP-2020 instrument. The typical amount of sample was 200 mg. The CO adsorption studies consisted of two consecutive isotherms, *P*(CO) range: 0–300 torr, with 30 min evacuation, at 308 K, in between. Prior to the experiment, the samples (Au/CZ-MD, Au/CZ-HD, CZ) were heated in a flow of 5% O_2/He, at 523 K (1 h), followed by 1 h evacuation at 523 K.

The deuterium spillover studies were carried out by using FTIR spectroscopy. Spectra were recorded in the transmission mode on a Bruker, Vertex 70, instrument equipped with a deuterated triglycine sulphate (DTGS) detector. Typically, 100 scans at a resolution of 4 cm^{-1} were averaged. In our study, a single self-supported wafer of 13 mm diameter was used. It was prepared by pressing 40 mg of the fresh catalyst powder at 5 ton cm^{-2} . The disk was placed in a transmission infrared quartz cell, with CaF_2 windows, which could be attached to a metallic high-vacuum manifold equipped with a turbo molecular pump (residual pressure $<10^{-6}$ torr). The sample disk was first submitted to our standard cleaning routine consisting of 1 h heating at 523 K, under flowing 5% O_2/He, followed by 1 h evacuation at 523 K; then, it was treated with CO (40 torr) for 1 h at 298 K; it was further evacuated for 30 min at 298 K, and finally, it was treated with D_2 (40 torr) for 1 h at 298 K. During the last step of the treatment a series of time-resolved spectra were recorded every 5 min. After completing this experiment, the sample was submitted again to the standard cleaning routine, and then treated with D_2 (40 torr) for 1 h at 298 K. Spectra were recorded under deuterium pressure every 5 min.

Acknowledgements

Financial support from MICIIN-Spain/FEDER-EU (projects MAT2008-00889-NAN and CSD2009-00013), the Junta de Andalucía (groups FQM-110 and FQM-334), and EU (contract 025995 (RITA) CENTACAT) are acknowledged. STEM-HAADF images were recorded at the SCCyT of the University of Cadiz.

[1] S. Carrettin, P. Concepcion, A. Corma, J. M. Lopez Nieto, V. F. Puntes, *Angew. Chem.* **2004**, *116*, 2592–2594; *Angew. Chem. Int. Ed.* **2004**, *43*, 2538–2540.

[2] J. Guzman, S. Carrettin, A. Corma, *J. Am. Chem. Soc.* **2005**, *127*, 3286–3287.

[3] A. M. Venezia, G. Pantaleo, A. Longo, G. Di Carlo, M. P. Casaletto, F. L. Liotta, G. Deganello, *J. Phys. Chem. B* **2005**, *109*, 2821–2827.

[4] D. Widmann, R. Leppelt, R. J. Behm, *J. Catal.* **2007**, *251*, 437–442.

[5] G. J. Hutchings, *Dalton Trans.* **2008**, 5523–5536.

[6] Z. Zhou, S. Kooi, M. Flytzani-Stephanopoulos, H. Saltsburg, *Adv. Funct. Mater.* **2008**, *18*, 2801–2807.

[7] I. Dobrosz-Gómez, I. Kocemba, J. M. Rynkowski, *Appl. Catal. B* **2008**, *83*, 240–255.

[8] I. Dobrosz-Gómez, I. Kocemba, J. M. Rynkowski, *Catal. Lett.* **2009**, *128*, 297–306.

[9] I. Dobrosz-Gómez, I. Kocemba, J. M. Rynkowski, *Appl. Catal. B* **2009**, *88*, 83–97.

[10] X. S. Huang, H. Sun, L. C. Wang, Y. M. Liu, K. N. Fan, Y. Cao, *Appl. Catal. B* **2009**, *90*, 224–232.

[11] H. Sakurai, T. Akita, S. Tsubota, M. Kiuchi, M. Haruta, *Appl. Catal. A* **2005**, *291*, 179–187.

[12] C. H. Kim, L. T. Thompson, *J. Catal.* **2005**, *230*, 66–74.

[13] R. Burch, *Phys. Chem. Chem. Phys.* **2006**, *8*, 5483–5500.

[14] R. Leppelt, B. Schumacher, V. Plzak, M. Kinne, R. J. Behm, *J. Catal.* **2006**, *244*, 137–152.

[15] W. Deng, M. Flytzani-Stephanopoulos, *Angew. Chem.* **2006**, *118*, 2343–2347; *Angew. Chem. Int. Ed.* **2006**, *45*, 2285–2289.

[16] Y. Denkwitz, A. Karpenko, V. Plzak, R. Leppelt, B. Schumacher, R. J. Behm, *J. Catal.* **2007**, *246*, 74–90.

[17] A. Karpenko, Y. Denkwitz, V. Plzak, J. Cai, R. Leppelt, B. Schumacher, R. J. Behm, *Catal. Lett.* **2007**, *116*, 105–115.

[18] A. Goguet, R. Burch, Y. Chen, C. Hardacre, P. Hu, R. W. Joyner, F. C. Meunier, B. S. Mun, D. Thompsett, D. Tibiletti, *J. Phys. Chem. B* **2007**, *111*, 16927–16933.

[19] W. Deng, A. I. Frenkel, R. Si, M. Flytzani-Stephanopoulos, *J. Phys. Chem. B* **2008**, *112*, 12834–12840.

[20] R. Si, M. Flytzani-Stephanopoulos, *Angew. Chem.* **2008**, *120*, 2926–2929; *Angew. Chem. Int. Ed.* **2008**, *47*, 2884–2887.

[21] A. Abd El-Moemen, A. Karpenko, Y. Denkwitz, R. J. Behm, *J. Power Sources* **2009**, *190*, 64–75.

[22] Y. Hao, M. Mihaylov, E. Ivanova, K. Hadjiivanov, H. Knoezinger, B. C. Gates, *J. Catal.* **2009**, *261*, 137–149.

[23] M. Lopez-Haro, J. J. Delgado, J. M. Cies, E. del Rio, S. Bernal, R. Burch, M. A. Cauqui, S. Trasobares, J. A. Perez-Omil, P. Bayle-Guillemaud, J. J. Calvino, *Angew. Chem.* **2010**, *122*, 2025–2029; *Angew. Chem. Int. Ed.* **2010**, *49*, 1981–1985.

[24] D. C. Meier, V. Bukhtiyarov, D. W. Goodman, *J. Phys. Chem. B* **2003**, *107*, 12668–12671.

[25] A. Carlsson, A. Puig-Molina, T. V. W. Janssens, *J. Phys. Chem. B* **2006**, *110*, 5286–5293.

[26] A. A. Herzing, C. J. Kiely, A. F. Carley, P. Landon, G. J. Hutchings, *Science* **2008**, *321*, 1331–1335.

[27] J. C. González, J. C. Hernandez, M. Lopez-Haro, E. del Rio, J. J. Delgado, A. B. Hungria, S. Trasobares, S. Bernal, P. A. Midgley, J. J. Calvino, *Angew. Chem.* **2009**, *121*, 5417–5419; *Angew. Chem. Int. Ed.* **2009**, *48*, 5313–5315, S5313/1.

[28] S. J. Pennycook, D. E. Jesson, *Ultramicroscopy* **1991**, *37*, 14–38.

[29] S. E. Collins, J. M. Cies, E. del Rio, M. Lopez-Haro, S. Trasobares, J. J. Calvino, J. M. Pintado, S. Bernal, *J. Phys. Chem. C* **2007**, *111*, 14371–14379.

[30] M. Nolan, S. Grigoleit, D. C. Sayle, S. C. Parker, G. W. Watson, *Surfactant Sci. Ser.* **2005**, *576*, 217–229.

[31] G. Jacobs, P. M. Patterson, U. M. Graham, D. E. Sparks, B. H. Davis, *Appl. Catal. A* **2004**, *269*, 63–73.

[32] A. Fonseca, J. Fisher, D. Ozkaya, M. Shannon, D. Thompsett, *Top. Catal.* **2007**, *44*, 223–235.

Received: April 7, 2010
Published online: June 22, 2010

